Large-angle magnetization dynamics measured by time-resolved ferromagnetic resonance

Th. Gerrits, M. L. Schneider, A. B. Kos, and T. J. Silva

National Institute of Standards and Technology, Boulder, Colorado 80305, USA

A time-resolved ferromagnetic resonance technique was used to investigate the nonlinear magnetization dynamics of a 10 nm thin Permalloy^{TM} film in response to a sequence of large-amplitude field pulses. The magnetic field pulse sequence was set at a repetition rate equal to the magnetic system's resonance frequency. Both inductive and optical techniques were used to observe the resultant magnetization dynamics. We compared data obtained by this technique with conventional pulsed inductive microwave magnetometry. The results for damping and frequency response obtained by these two different methods coincide in the limit of a small-angle excitation. However, when applying large-amplitude field pulses, there was a substantial increase in the apparent damping. Analysis of vector-resolved magnetic second-harmonic generation data indicate that the increase in damping is correlated with a decrease in the spatial homogeneity of the magnetization dynamics. This suggests that unstable spin wave generation occurs in the limit of large-amplitude dynamics.

I. INTRODUCTION

Recently, there have been several investigations of high-speed, large-angle magnetization dynamics in thin film systems using various time-resolved methods.[1–3] These time-resolved investigations have been motivated in part by the inability to make such large-angle measurements using cw ferromagnetic resonance (FMR) techniques. In the case of FMR, pumping beyond the instability threshold results in the unstable generation of spin waves (i.e., the Suhl instability), thereby causing a collapse of the ac susceptibility on resonance.[4] It appears that time-resolved techniques are not susceptible to the Suhl instability,[5] thereby permitting investigations of dynamical properties at large precession angles.

The speed of the magnetization response in thin films results from the large demagnetization factor associated with the magnetization component in the surface normal direction. The role of the demagnetizing factors in establishing the precession frequency ω in the small-angle limit is formulated in terms of the Kittel equation. For a thin film, the Kittel equation reduces to $\omega = \gamma \mu_0 \sqrt{(M_s + H_k + H_b)(H_k + H_b)}$, where γ is the gyromagnetic ratio, μ_0 is the permeability of free space, M_s is the saturation magnetization, H_k is the uniaxial anisotropy, and H_b is the applied dc bias field along the easy axis direction. This suggests that high-frequency, large-angle, steady-state dynamics may be observable in certain experimental geometries where the demagnetizing field is actually the principle source of magnetic field that drives the magnetization precession. Such a possibility is reinforced by recent results for dynamics generated by spin momentum transfer effects.

Recent studies of spin-torque-induced dynamics in nanopillar structures with in-plane applied fields have shown the existence of a "self-biased" state at large currents where the magnetization precesses about a self-induced demagnetizing field in the surface normal direction.[6] In such a self-biased state, the demagnetizing field is the principle source of the magnetic field that drives the magnetization precession. The frequency of precession in the self-biased state is primarily a

function of the perpendicular component of magnetization such that $\omega \approx \gamma \mu_0 M_z = \gamma \mu_0 M_s \cos \theta$, where θ is the cone angle of precession relative to the surface normal. The dynamics for such a state are inherently nonlinear since the frequency of precession now depends explicitly on the amplitude of precession through the dependence on θ.[7,8] The present study was motivated by the interest in determining if self-biased dynamical states could be achieved in a macroscopic time-resolved measurement using a finite duration burst of cw microwave radiation to initiate the large-angle dynamics.

We report on the magnetization dynamics initiated by small- and large-amplitude time-resolved ferromagnetic resonance (TR-FMR). We define TR-FMR as the excitation of a magnetic system by a sequence of magnetic field pulses with a repetition rate that is close or equal to the resonance frequency of the magnetic system under study, and the detection of the resultant dynamics using time-resolved methods. Here, we use both an inductive detection technique, similar to that employed in a pulsed inductive microwave magnetometer (PIMM),[1] and time-resolved magnetic second-harmonic generation to acquire the TR-FMR signal. A sequence of magnetic field pulses (ranging from 1 to 16 pulses) was used to investigate the magnetodynamics in a thin Permalloy^{TM} (Ni$_{80}$Fe$_{20}$) film. This sequence of pulses was generated by a commercial pulse/data pattern generator. In this way we could directly compare the TR-FMR (comparable to conventional FMR when the number of pulses is large) and the conventional PIMM-method (which makes use of a single-step magnetic field pulse). We show that TR-FMR and PIMM yield the same results, regardless of the number of pulses in the sequence, for the extracted damping parameter and frequency response of the sample under investigation in the limit of small-angle excitations. However, for large-amplitude excitations that should be sufficient to induce self-biased dynamics, the apparent damping is enhanced by a factor of 5 compared to the PIMM and small-amplitude TR-FMR results. The enhanced damping prevents the formation of a self-biased state in these experiments. The
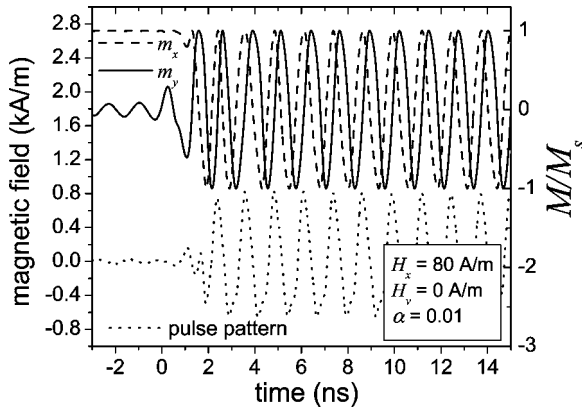
FIG. 1. Landau-Lifshitz simulation of thin Permalloy™ film response due to a pulse field pattern (dotted line). The solid line shows the component of the magnetization along the y axis and the dashed line shows the component along the x axis. The parameters for the simulation are given in the lower inset.

FIG. 2. The experimental configuration as used throughout this study. The easy axis of the sample is always parallel to the x axis and the pulse field is always applied along the y axis. The bias field may be applied along both the x and the y axes. Trajectory "A" is that for small amplitude elliptical precession in response to a weak ac field. Trajectory "B" is for a self-biased state where the magnetization precesses about the quasistatic demagnetizing field along the z axis.

data suggest that this enhanced damping is the result of non-linear instabilities that lead to parametrically pumped spin wave generation.

Figure 1 shows a simulation of a self-biased precessional state for a thin Permalloy™ film due a large-amplitude field pulse sequence (dotted line). The repetition rate of the field pulse sequence was equal to 786 MHz. The dashed and solid lines in Fig. 1 represent the two in-plane components of the magnetization for a thin Permalloy ($Ni_{80}Fe_{20}$) film, calculated with a Landau-Lifshitz macrospin model.[9] For this simulation, we chose a static bias field H_{bx} of 80 A/m (1.0 Oe), a uniaxial anisotropy field $H_k^{(2)}$ of 600 A/m (7.55 Oe) and a damping parameter α of 0.01. The pulse pattern had peak-to-peak amplitude of 1.5 kA/m (19 Oe). This macrospin simulation clearly shows a 90° phase shift between the x and y components of the magnetization indicating that the magnetization follows a continuous 360° in-plane rotation mode after the first cycle of the pulse sequence. This continuous rotational mode is synchronous with the applied field for the duration of the remaining pulse sequence. The synchronization mechanism is characterized by a nearly constant out-of-plane component of the magnetization $\vec{M}$. The out-of-plane component of $\vec{M}$ results in a de-magnetizing field that increases the rotation frequency of $\vec{M}$ in proportion to the tilt angle of the magnetization, i.e., self-biasing occurs due to the constant out-of-plane component. As a result, $\vec{M}$ can be synchronized to the external frequency source even when the driving frequency is slightly higher than the film's natural resonance frequency for small-angle motion about the equilibrium axis.

Despite the fact that single-domain simulations show the possibility of exciting a continuous rotation mode in response to a finite sequence of large amplitude field pulses, we will show that we were not able to detect a self-biasing of the magnetization in a 360° rotation mode by TR-FMR in a quasi-infinite thin Permalloy™ film. Vector-resolved data suggest that $\vec{M}$ undergoes a highly nonlinear process, comparable to the Suhl instability,[10] which prevents the self-biased state from being established.

II. EXPERIMENT

Figure 2 shows the field geometry used throughout this study. The excitation field H_p is always applied along the y axis and the uniaxial anisotropy easy axis of the magnetic sample lies along the x axis. Static magnetic bias fields H_{bx} and H_{by} can be applied along both the x and y axes, respectively. We used a commercial pulse/pattern generator with a bandwidth of 3.3 GHz to produce the excitation pulse sequences. The pattern generator was capable of generating a 32-bit burst data pattern with a maximum output voltage of 3.3 V. In order to achieve large-amplitude field pulses, the pulse pattern was externally amplified by 30 dB. The minimum "bit" length was limited to 286 ps. The maximum "bit" length was 30 ns. The pattern generator was capable of applying TR-FMR pulse patterns of up to 16 pulses with a 50% duty cycle and variable repetition frequency. The pulse pattern was launched into a coplanar waveguide structure with 110 μm center conductor width, yielding a maximum H_p of 1.5 kA/m (19 Oe), peak-to-peak. The dotted line in Fig. 1 shows a representative experimental pulse pattern with a repetition rate of 786 MHz, measured with a sampling oscilloscope and converted to units of magnetic field by use of the Karlqvist equation.[11]

We measured the small-angle response using the PIMM. The PIMM is a nonlocal broadband instrument and therefore stroboscopically measures the average response of the complete excited sample. Further details on the PIMM and data analysis technique can be found in earlier work by Silva *et al.*[1] and Alexander *et al.*[12]

The large-angle response was measured utilizing the time-resolved magnetization-induced optical second-harmonic generation (MSHG). MSHG is sensitive to the different components of in-plane magnetization and therefore allows extraction of the deflection angle and absolute value of $\vec{M}$.[13,14] Our measured value for $|\vec{M}|$ is spatially averaged over the optical spot size of approximately 10 μm, and is a measure of the coherence of the magnetization motion at the length scale of the probe size.[15] Thus, determination of $|\vec{M}|$ allows us to infer nonlinearity (i.e., generation of spin waves) during large-angle deflections.

To improve our signal-to-noise ratio, the data for $|\vec{M}|$ were temporally filtered with a running average over a 2.4 ns wide window, decreasing the effective bandwidth of the magnitude data to 200 MHz. The data for the deflection angle were not filtered.

The MSHG system uses a mode-locked Ti:sapphire laser, producing 100 fs optical pulses that generate second-harmonic light upon reflection from a metallic surface. The repetition rate of the laser pulses is fixed to the laser's cavity length and is about 82 MHz. The repetition rate of the laser pulses was set by an external pulse picker to about 10 MHz. In order to achieve time resolution, the pattern generator was synchronized to the laser oscillator using a phase-lock loop.

The sample was a 10 nm Permalloy™ ($Ni_{80}Fe_{20}$) film with a 5 nm Ta capping layer to prevent oxide formation at the Permalloy surface. The sample was dc magnetron sputtered directly onto a glass substrate. The glass substrate was etched with Ar/O_2 and Ar ion milling to improve adhesion prior to the deposition of the Permalloy film. We deposited Permalloy at an Ar pressure of 0.53 Pa (4.0 mTorr). The Ta was sputtered at an Ar pressure of 0.67 Pa (5.0 mTorr).

III. RESULTS

In the following sections, we will present the results obtained by conventional PIMM, small-angle inductive TR-FMR, and large-angle optical TR-FMR using a single thin-film sample.

Small-amplitude response

We first measured the response of the magnetic film to a single small magnetic field step by use of the PIMM. The step-excitation amplitude was 60 A/m (0.8 Oe) for these measurements. From the free induction data, we could determine the resonance frequency, dynamic anisotropy field, and the damping parameter as a function of bias field.[1,12] The precession frequency was varied by adjusting the applied bias field. The dynamic anisotropy field of the sample was found to be 620±20 A/m (7.7±0.2 Oe), which is 160 A/m (2 Oe) higher than the static uniaxial anisotropy. This indicates that a rotatable component of anisotropy is present in the sample, in agreement with earlier studies.[16,17] The normalized relaxation rate $2/\tau\omega_m$, where $\omega_m = \gamma\mu_0 M_s$, is extracted from the measured relaxation time τ of the free induction decay. In the absence of any additional relaxation mechanisms besides intrinsic damping, $2/\tau\omega_m$ is equivalent to the Gilbert damping parameter α. The normalized relaxation rate is plotted in Fig. 3 as a function of precession frequency (filled upside-down triangles). At low frequencies, the relaxation rate increases as shown in earlier studies.[15,18–20]

The frequency response obtained from the PIMM measurements was used to set the field pulse pattern repetition rate for small amplitude TR-FMR measurements with H_p =60 A/m (0.8 Oe). We then measured the sample response by inductive TR-FMR for H_{bx}=240 A/m (3 Oe), 480 A/m (6 Oe), 720 A/m (9 Oe), and 1.2 kA/m (15 Oe), and H_{by} set to zero. Figure 4 shows the response of the thin
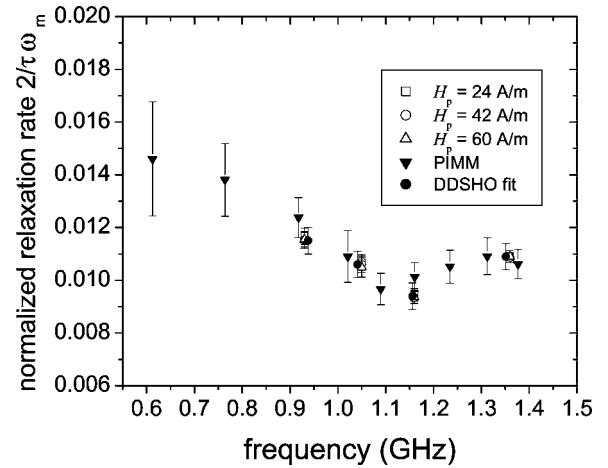
FIG. 3. Extracted normalized relaxation rate as a function of frequency from PIMM measurements (down triangles). The solid circles show the normalized relaxation rate extracted from the fits to the driven damped simple harmonic oscillator model. All open symbols represent the extracted normalized relaxation rate from the free induction decay after the field pulse sequence was turned off.

film when excited by a sequence of 16 field pulses with a repetition rate of 1.16 GHz and for H_{bx}=720 A/m(9 Oe). The data were fit to a driven damped simple harmonic oscillator model at the oscillator resonance. The time required for the system to reach steady state is inversely proportional to the damping. The fit is in good agreement with the data and yields a relaxation rate that can be expressed in terms of a Gilbert damping parameter α=0.0094±0.0005 and a dynamic anisotropy field H_k of 590±10 A/m(7.4±0.1 Oe). The fitted anisotropy is in good agreement with the values obtained by conventional PIMM. For all four bias fields, the value for the extracted anisotropy ranges from 570±10 A/m(7.2±0.1 Oe) to 620±10 A/m(7.8±0.1 Oe). Additional extracted values of the relaxation rate for all four bias fields are given by the solid dots in Fig. 3. We verified
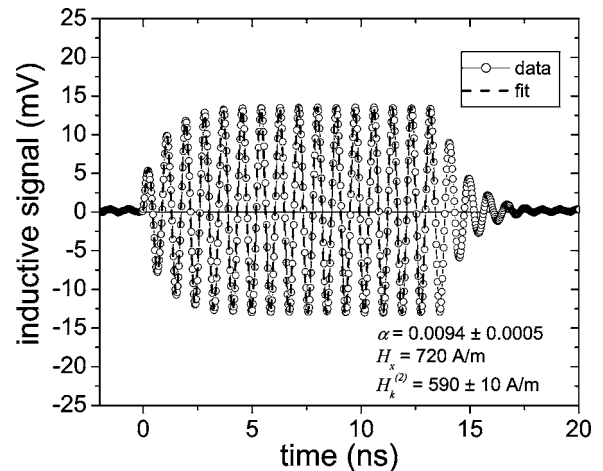
FIG. 4. Time-resolved ferromagnetic resonance for a 10 nm thin Permalloy™ film, measured with the inductive technique. The dashed line represents the driven damped simple harmonic oscillator fit.

that the fitted parameters were insensitive to pulse amplitude for $H_p < 60$ A/m(0.8 Oe).

We also investigated whether the number of generated field pulses has any effect on the relaxation rate of the system when the pulse sequence is turned off. We used three different pulse amplitudes and pulse sequences ranging from one pulse up to a sequence of 16 pulses. The three pulse amplitudes H_p were 24 A/m(0.3 Oe), 42 A/m(0.5 Oe) and 60 A/m(0.8 Oe), calculated using the Karlqvist equation.[11] The extracted relaxation rate did not show any significant change when the number of pulses was changed. In addition, the relaxation rates were also insensitive to the different pulse amplitudes, shown by the open symbols in Fig. 3. Figure 3 shows that the relaxation rates obtained by both, the conventional PIMM and the TR-FMR technique are similar. This stems from a uniform magnetization motion during these small-angle excitations. Because the extracted relaxation rates have the same value in the small angle limit, we may also speculate that the relaxation rate will be the same for both an infinite number of pulses (conventional FMR) and single pulse (PIMM) measurements. Indeed, work in progress indicates that conventional FMR and PIMM measurements of damping in thin Permalloy™ films are in agreement.[21]

IV. LARGE-AMPLITUDE RESPONSE

In the following section we will discuss the results of magnetization dynamics generated by large-amplitude magnetic field pulse patterns of 1.5 kA/m(19 Oe), peak-to-peak. In order to determine whether a large-angle motion or even a full 360° rotation occurs, a magnetization vector-resolved technique must be utilized. However, inductive techniques cannot measure the dynamics of the magnetization vector. Thus, we used time- and vector-resolved magnetization-induced optical second-harmonic generation (MSHG) to measure the large-angle dynamics.[13]

Figure 5 shows the data for a vector-resolved MSHG measurement. The bias fields were $H_{bx} = 220$ A/m(2.75 Oe) and $H_{by} = 0$ A/m, respectively. The squares are the magnetization angle relative to the x axis. The open circles are $|\vec{M}|$ normalized to the saturation magnetization. The dashed and dotted lines in Fig. 5 are the results from two macrospin simulations that utilize the pulse pattern shown in Fig. 1 as the driving term. A uniaxial anisotropy field $H_k^{(2)}$ of 440 A/m(5.5 Oe) and a rotational anisotropy field $H_k^{(0)}$ of 160 A/m(2 Oe)were used for the simulations. For this particular combination of bias fields and anisotropy fields simulations predicted that the system would not enter a self-biased state. Indeed, the data confirm this prediction. However, using a damping of $\alpha = 0.013$, the simulation results shown in Fig. 5 as a dashed line are in poor agreement with the data. The data show that the magnetization remains confined to a smaller precession cone than what is predicted with the simulations. It was necessary to increase the damping parameter to a value in the range of $0.045 < \alpha < 0.055$ to get reasonable agreement between the simulations and the data. The need for such a large damping parameter to fit the
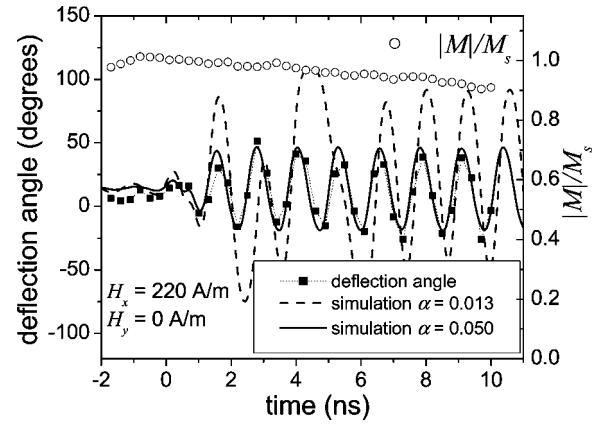
FIG. 5. Vector-resolved large-angle excitation response, as measured by MSHG. The open circles are the normalized absolute value of the magnetization. The data for the magnetization value were low-pass filtered with a bandwidth of 200 MHz to improve the signal-to-noise ratio. The solid squares show the magnetization deflection angle relative to the x direction. The dashed and solid lines are the results of Landau-Lifschitz-Ginsburg (LLG) simulations for damping parameters of 0.013 and 0.050, respectively.

data suggests that the dynamics are no longer well described with a macrospin model, as we will discuss in more detail below.

None of the bias field combinations that we tested resulted in the formation of a self-biased state. In addition, the damping parameter needed to fit the measured dynamics was in the range $0.045 < \alpha < 0.055$, independent of the applied bias fields. Figure 6 shows the dynamics for the particular bias field combination of $H_{bx} = 120$ A/m(1.5 Oe) and $H_{by} = 170$ A/m(2.2 Oe). For this particular bias field combination, one would expect a 360° in-plane rotation after the first few cycles of the pulse sequence based on our simulations using the macrospin model with $\alpha = 0.013$. In addition, the data in Fig. 6 also show a strong decrease of $|\vec{M}|$ to a value of
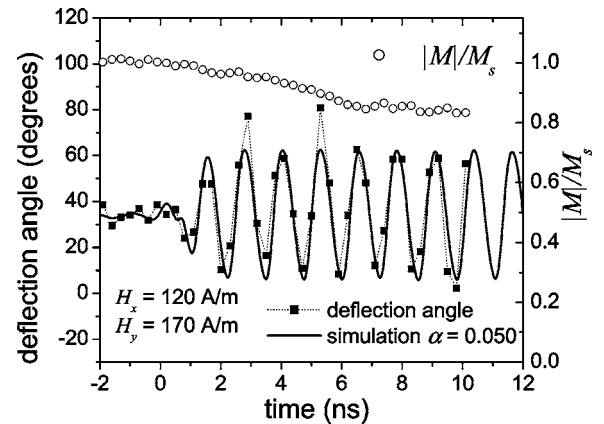
FIG. 6. Vector-resolved large-angle excitation measured by MSHG. The open circles represent the normalized absolute value of the magnetization. The data for the magnetization value were filtered down to a bandwidth of 200 MHz for the sake of clarity. The squares show the magnetization deflection angle from the x direction. The solid line shows the LLG simulation for $\alpha = 0.050$.
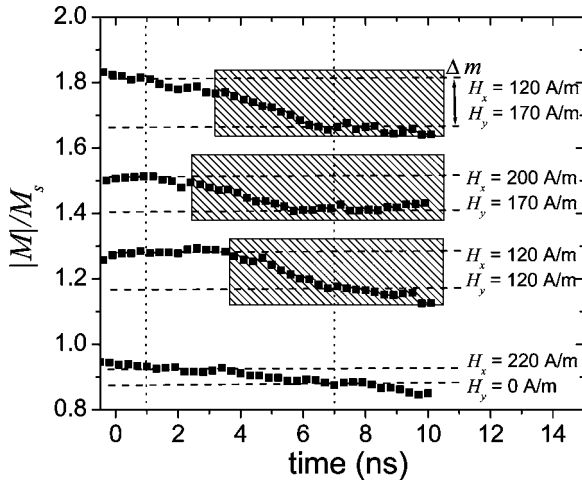
FIG. 7. Solid squares show the absolute value of the magnetization for various bias field combinations. The data were low-pass filtered down to 200 MHz, indicating a drop in the normalized absolute value of $\vec{M}$. The determination of Δm was done by determination of the adjacent average values of $|\vec{M}|$ at 1 ns and at 7 ns (dashed lines). The hatched areas represent the 360° locking state of the magnetization, calculated by the LLG model with a damping parameter of 0.013. Note that the graphs are plotted in a waterfall plot. The data are shifted upwards by $n(0.25)|\vec{M}|/M_s(n=0,1,2,3)$ for the sake of clarity.

about 0.8 Ms in response to the field pulse sequence.

A similar decrease in $|\vec{M}|$ over the course of the field pulse sequence occurred for other bias field combinations, as can be seen in Fig. 7. The graph shows a waterfall plot of $|\vec{M}|$ as a function of time for various bias field combinations. We designate $|\vec{M}|$ at $t=1$ ns (just after the onset of the pulse sequence) and at $t=7$ ns, as the initial and steady-state magnetization values, respectively. $|\vec{M}|$ does not appear to change any further for $t>7$ ns. The magnetization difference, Δm, between steady-state and initial magnetization values are 15%, 9%, 11%, and 4% for the data sets, shown from top to bottom. The first three bias field settings are all expected to exhibit self-biased states based upon our simulations. The data sets associated with the same bias fields all show a substantial magnetization decrease $\Delta m > 9\%$. The last bias field set of $H_{bx}=220$ A/m, $H_{by}=0$ did not result in a self-biased state in simulations. The associated data set also exhibited the smallest magnetization decrease of $\Delta m=4\%$. The hatched areas represent the time intervals where macrospin simulations with $\alpha=0.013$ predict that the magnetization should be in a self-biased state. The moment in time when $\vec{M}$ is expected to enter a self-biased state roughly coincides with the time when $|\vec{M}|$ actually starts to decrease in the measurements. The enhancement of the apparent damping, as well as the reduction of $|\vec{M}|$, both suggest that the dynamics in these experiments are characterized by the unstable growth of spin wave modes when the sample is subjected to large-amplitude pulse sequences.

V. DISCUSSION

Further theoretical consideration supports our hypothesis that the difference in behavior for small-amplitude versus large-amplitude TR-FMR experiments is due to spin wave instabilities. While spin wave instabilities have been clearly observed for large-amplitude FMR experiments with Permalloy™ films,[22] the field pulse amplitudes used for the small-amplitude measurements reported here are marginally below the theoretical threshold for resonance saturation (i.e., the second-order spin wave instability) for all combinations of pump and bias field amplitudes. We need not consider the first-order instability since the pump field employed here is always at the resonance frequency of the uniform mode. The first-order instability, also known as subsidiary absorption, is most often of concern when pumping off resonance. That we are below the threshold for nonlinear spin wave generation may be easily shown using common expressions for the spin wave instability. The threshold pump field amplitude H_{pt} for the second-order instability may be approximated as[4]

$$H_{pt} = \Delta H \left(\frac{2\Delta H_k}{M_s} \right)^{1/2}, \tag{1}$$

where ΔH and ΔH_k are the field linewidths for the uniform and degenerate magnon modes, respectively. Using the Landau-Lifshitz model for the dynamics, and assuming that the damping for degenerate spin waves is the same as for the uniform mode, we find that

$$\Delta H_{(k)} = \frac{2\alpha\omega}{\gamma\mu_0}. \tag{2}$$

Substituting Eq. (2) into Eq. (1), and then converting to a threshold angle θ_t for the in-plane precession, we arrive at

$$\theta_t = \sqrt{\frac{\alpha}{2}} \chi_0 \left(\frac{2\omega}{\omega_M} \right)^{5/2}, \tag{3}$$

where χ_0 is the dc susceptibility and $\omega_M \doteq \gamma\mu_0 M_s$. Using Eq. (3), the threshold angle θ_t is calculated to be 5° at the highest frequencies used in the small-amplitude measurements. The estimated experimental in-plane precession angle is 4.0° for resonant pumping with a peak-to-peak pump field H_p $=60$ A/m(0.8 Oe) and a bias field $H_{bx}=1.2$ kA/m(15 Oe). Since the onset of premature saturation would have manifested itself as a dependence of the apparent damping on pump amplitude, we conclude that the instability for parametric spin wave generation is not operative in our low-amplitude experiments.

It was previously shown that spin wave instabilities are not evident in PIMM studies that employ a single-step excitation even for pulse excitations well in excess of the second-order instability threshold.[5] This is not surprising in the case of single-pulse excitations at low bias fields since the parametric pumping of derivative spin wave modes requires the continuous application of a microwave field that drives the dynamics. This can be qualitatively understood in terms of a simple rate equation for the spin wave population. If $N_{\bar{k}}$ be

the zero-temperature magnon density at wave vector $\vec{k}$, then the nonlinear magnon population dynamics near the instability threshold may be simply described by[10]

$$\frac{dN_{\vec{k}}}{dt} \approx -\lambda_{\vec{k}}\left[1 - \left(\frac{2P(\vec{k}\approx 0)}{P_{th}} - 1\right)^{1/2}\right]N_{\vec{k}}, \qquad (4)$$

where $\lambda_{\vec{k}}$ is the magnon decay rate, $P(\vec{k}\approx 0)$ is the pump power for the uniform mode, and P_{th} is the threshold pump power for the spin wave instability. For $P(\vec{k}\approx 0) > P_{th}$, the magnon density grows exponentially and the system is unstable. In a conventional cw FMR experiment, $P(\vec{k}\approx 0)$ is essentially constant over time. However, in a time-resolved single-pulse excitation experiment, the dynamics are instigated by a sudden reorientation of the equilibrium magnetization direction. In such a broadband experiment, all possible modes that are accessible within the spatial and temporal bandwidth of the pulsed field source are excited.[17] However, none of the excited modes are actually *pumped*; an initial short burst of energy ΔE is delivered to a multiplicity of modes, but none of the modes are driven in a manner that allows for the parametric pumping of degenerate spin wave modes. In terms of Eq. (4), $P(\vec{k}\approx 0)$ is nonzero only on a time scale short compared to the precession period in the case of free induction decay, i.e., $P(\vec{k}\approx 0;t)\approx\Delta E\delta(t)$. Even in the case that $\Delta E \gg E_{th}$, the magnon population dynamics remain stable after the application of the field pulse for most experimental geometries. The exception to this rule is in the case of a transversely biased, free induction decay experiments, which is discussed in more detail below.

It is only in the case of oscillatory pumping that any additional damping due to spin wave generation was observed. While this result is not surprising in itself, since the pumping amplitude was far in excess of the instability threshold for the large amplitude studies presented here, what is of note is how quickly the nonlinear effects act to substantially increase the viscosity of the observed magnetization dynamics. Though it takes 3 ns for the system to arrive at steady state for the small amplitude dynamics shown in Fig. 4, it only takes 1.5 ns for the same system to display the highly viscous response shown in Figs. 5 and 6. This implies that only one full period of microwave radiation is required to instigate any spin wave instabilities. The rapid onset of the nonlinear behavior can be understood in terms of the particular mode that we have attempted to excite. If the precession frequency in the case of continuous 360° in-plane rotation is predominantly a function of the perpendicular component of magnetization (as single domain simulations indicate), then any spatial variations in the mode amplitude will result in local fluctuations of the mode frequency, necessarily causing the magnetization distribution to become even more nonuni-

form. This is exactly the scenario for runaway spin wave growth that was considered in the original treatment by Anderson and Suhl.[10]

Similar considerations lead to a physical understanding of the rapid spin wave growth observed in Ref. 14 in the case of a small bias field applied along the hard axis of a Permalloy™ film. When the transverse bias field is approximately equal to the anisotropy, the linear restoring force acting on the magnetization is compensated and the mode dynamics are a strong function of mode amplitude. Thus, any magnetization dynamics generated in this special geometry are inherently unstable, leading to spin wave population growth even in the absence of any pumping field.

Such spin wave instabilities are not operative in SMT experiments even though it has been shown that the frequency of the excited modes depends strongly on mode amplitude.[23,24] In such experiments, the dynamics result from the regenerative amplification of persistent nonlinear self-oscillations.[25] This is in sharp contrast to FMR experiments because the observed limit cycles are not the product of resonant pumping, as is the case for FMR, but are instead the result of the local compensation of damping by the spin torque effect. As such, the instigation of magnetization dynamics in an SMT experiment is highly analogous to the population growth of higher order spin wave modes described by Eq. (4).

In summary, we were not successful in observing continuous, 360°, self-biased magnetization dynamics in time-resolved measurements, even though such modes are observed in single-domain simulations that utilize the dynamical parameters obtained from small amplitude resonant pumping experiments. The failure to excite such modes is understood in terms of the second-order spin wave instability that is usually observed in high-field-pumping FMR studies. Such instabilities would appear to be unavoidable in the experimental geometry that we have chosen, even though such instabilities do not limit either large-amplitude free induction decay experiments or microwave emissions from spin torque nano-oscillators. We conclude that the spin wave instability is not applicable in the absence of a cw microwave pumping field, as in the case of single-step PIMM studies, nor is the instability operative when the excited mode is regeneratively amplified, as is the case for SMT studies. However, the spin wave instability is a dominant effect in any experimental geometry where the resonantly pumped mode has a strong frequency dependence upon the mode amplitude.

[1] T. J. Silva, C. S. Lee, T. M. Crawford, and C. T. Rogers, J. Appl. Phys. **85**, 7849 (1999).

[2] Th. Gerrits, H. A. M. van den Berg, J. Hohlfeld, L. Bär, and Th. Rasing, Nature (London) **418**, 509 (2002).

[3] A. Krichevsky and M. R. Freeman, J. Appl. Phys. **95**, 6601 (2004).

[4] A. H. Morrish, in *The Physical Principles of Magnetism.* (IEEE Press, New York, 2001), pp. 578–588.

[5] J. P. Nibarger, R. Lopusnik, and T. J. Silva, Appl. Phys. Lett. **82**, 2112 (2003).

[6] S. I. Kiselev, J. C. Sankey, I. N. Krivorotov, N. C. Emley, A. G. F. Garcia, R. A. Buhrman, and D. C. Ralph, Phys. Rev. B **72**, 064430 (2005).

[7] A. N. Slavin and P. Kabos, IEEE Trans. Magn. **41**, 1264 (2005).

[8] M. A. Hoefer, M. J. Ablowitz, B. Ilan, M. R. Pufall, and T. J. Silva, Phys. Rev. Lett. **95**, 267206-1 (2005).

[9] T. L Gilbert, Phys. Rev. **100**, 1243 (1955), T. L. Gilbert, IEEE Trans. Magn. **40**, 3443 (2004).

[10] P. W. Anderson and H. Suhl, Phys. Rev. **100**, 1788 (1955).

[11] O. Karlqvist, Transactions of the Royal Institute of Technology, Stockholm **86**, 3 (1954).

[12] C. Alexander, J. Rantschler, T. J. Silva, and P. Kabos, J. Appl. Phys. **87**, 6633 (2000).

[13] Th. Gerrits, T. J. Silva, H. A. M. van den Berg, and Th. Rasing, Rev. Sci. Instrum. (submitted).

[14] T. J. Silva, P. Kabos, and M. R. Pufall, Appl. Phys. Lett. **81**, 1 (2002).

[15] Th. Gerrits, T. J. Silva, J. P. Nibarger, and Th. Rasing, J. Appl. Phys. **96**, 6023 (2004).

[16] R. Lopusnik, J. P. Nibarger, T. J. Silva, and Z. Celinski, Appl. Phys. Lett. **83**, (2003).

[17] M. L. Schneider, A. B. Kos, and T. J. Silva, Appl. Phys. Lett. **85**, 254 (2004).

[18] G. Counil, J. V. Kim, T. Devolder, C. Chappert, K. Shigeto, and Y. Otani, J. Appl. Phys. **95**, 5646 (2004).

[19] B. Kuanr, R. E. Camley, and Z. Celinski, Appl. Phys. Lett. **87**, 012502 (2005).

[20] M. Schneider, Th. Gerrits, A. B. Kos, and T. J. Silva, Appl. Phys. Lett. **87**, 072509 (2005).

[21] S. S. Kalarickal, M. Wu, P. Krivosik, C. E. Patton, M. L. Schneider, P. Kabos, T. J. Silva, and J. P. Nibarger, J. Appl. Phys. (to be published).

[22] S. Y. An, P. Krivosik, M. A. Kraemer, H. M. Olson, A. V. Nazarov, and C. E. Patton, J. Appl. Phys. **96**, 1572 (2004).

[23] W. H. Rippard, M. R. Pufall, S. Kaka, S. E. Russek, and T. J. Silva, Phys. Rev. Lett. **92**, 027201 (2004).

[24] S. I. Kiselev, J. C. Sankey, I. N. Krivorotov, N. C. Emley, R. J. Schoelkopf, R. A. Buhrman, and D. C. Ralph, Nature (London) **425**, 380 (2003).

[25] G. Bertotti, C. Serpico, I. D. Mayergoyz, A. Magni, M. d'Aquino, and R. Bonin, Phys. Rev. Lett. **94**, 127206 (2005).